SUPPORTING INFORMATION

Lysine Carbonylation is a Previously Unrecognized Contributor to Peroxidase Activation of Cytochrome *c* by Chloramine-T

Victor Yin, Safee H. Mian, and Lars Konermann*

Department of Chemistry, The University of Western Ontario, London, Ontario, N6A 5B7, Canada

* corresponding author

E-mail address of the corresponding author: konerman@uwo.ca

This file contains:

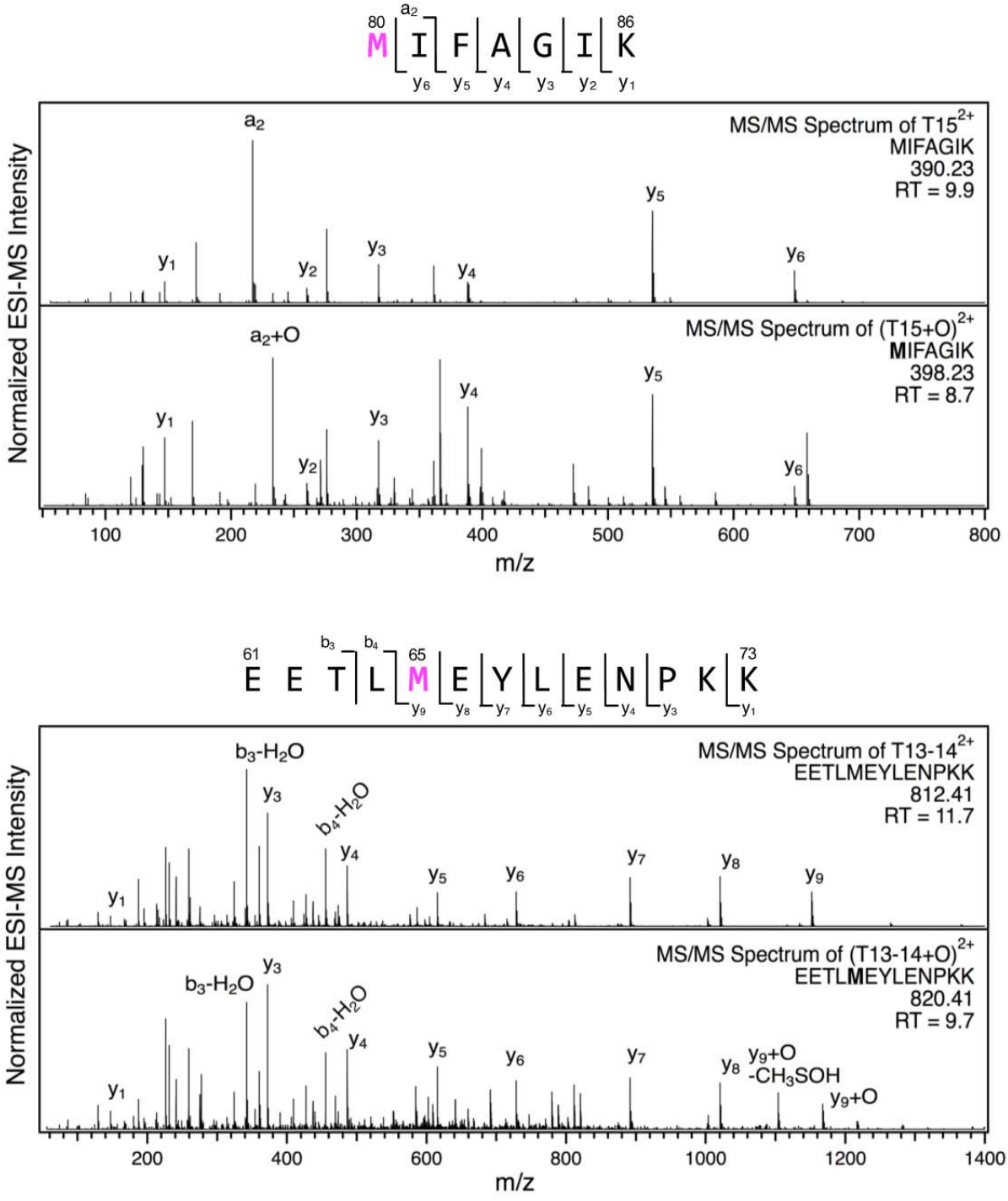

Fig. S1. Tandem mass spectra of Met-containing tryptic peptides. In each panel, the top trace depicts the unmodified peptide, whereas the bottom trace depicts the MetO form. Top: peptide T15 (residues 80-86) reveals (+16 Da) at Met80. Bottom: peptide T13-14 (residues 61-73), with MetO formation at Met65. These experiments were conducted on unfractionated samples. i.e., without prior SCX chromatography.

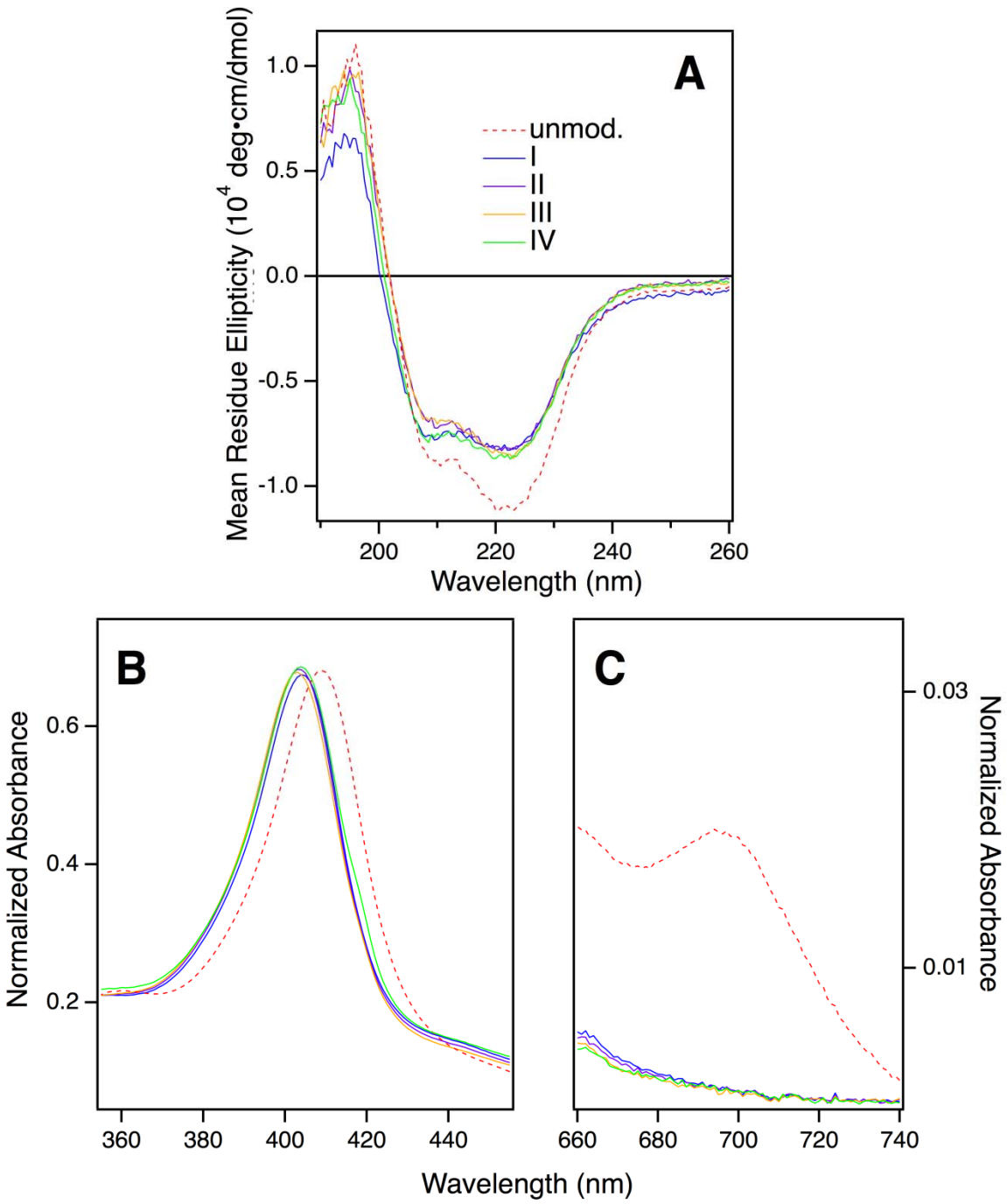

Fig. S2. Optical spectroscopy of CT-cyt *c* fractions. All data was compared against unmodified cyt *c* controls (dashed red trace) (A) Far-UV CD spectra. (B) Soret UV/vis to probe heme coordination environment. (C) A695 UV/vis band, characteristic of the Fe-Met80 bond.

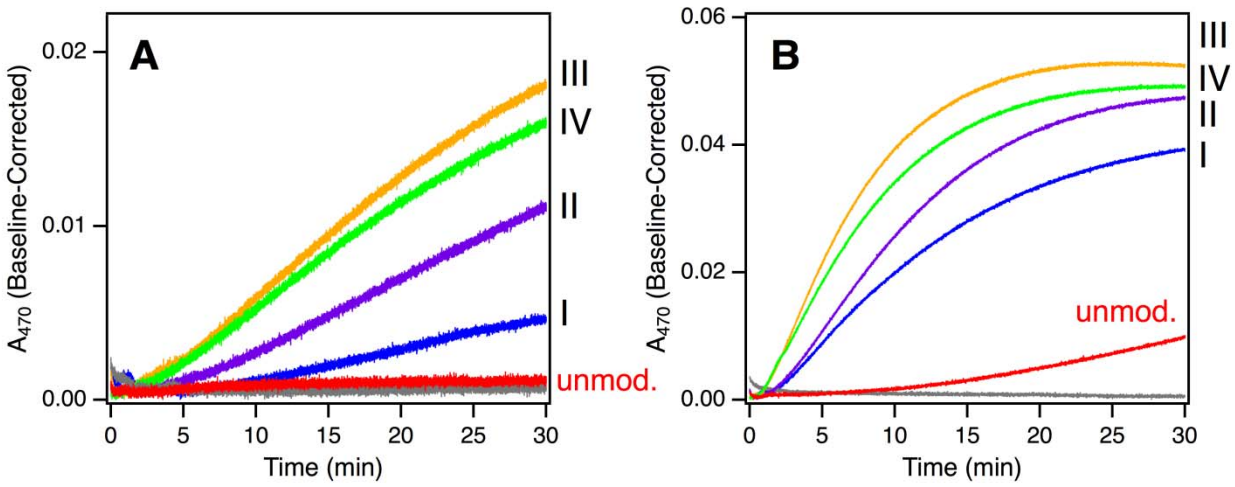

Fig. S3. (A): Peroxidase activity of CT-cyt *c* fractions detected by the oxidation of guaiacol in the presence of 100 µM H_2O_2. Rates were measured from the slope of the linear range, resulting in the activity data of Fig. 2B (main text). Also depicted are data for an unmodified cyt *c* control (red), and a control without protein (grey). (B) Same as in panel A, but at an increased H_2O_2 concentration of 500 µM. Note that the activity trends of the various fractions remained the same under both conditions. In panel B, a non-zero peroxidase activity with an initial lag phase of low activity was observed for unmodified cyt *c*, consistent with earlier observations.[1]

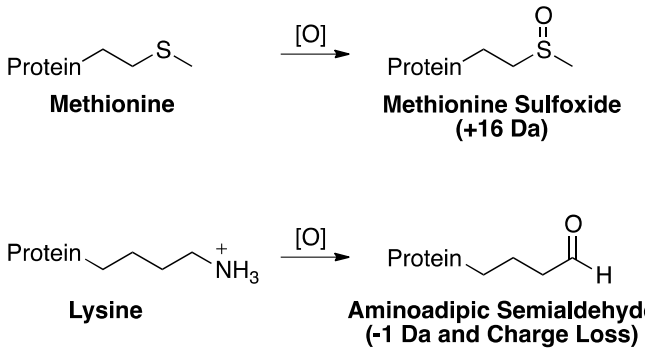

Fig. S4. Structures of oxidation products of methionine (MetO, methionine sulfoxide) and lysine (LysCHO, aminoadipic semialdehyde).

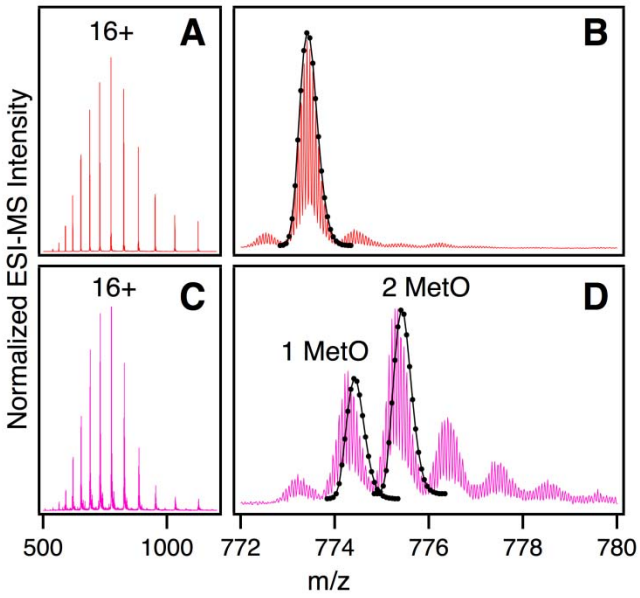

Fig. S5. Intact protein ESI mass spectra of cyt *c* before (red) and after (magenta) CT treatment, but prior to SCX fractionation. Panels A and C depict the total charge state envelope, where panels B and D show a magnified view of the 16+ charge state. The data for unmodified cyt *c* are overlaid with a simulated isotopic distribution, demonstrating excellent agreement. The CT-cyt *c* mass spectrum is overlaid with simulated isotopic distributions for Met oxidation (+16 and +32 Da, respectively). Major discrepancies are observable between simulated and experimental isotopic envelopes for CT-cyt *c*. These discrepancies are caused by the presence of LysCHO sites under the conditions of C/D.

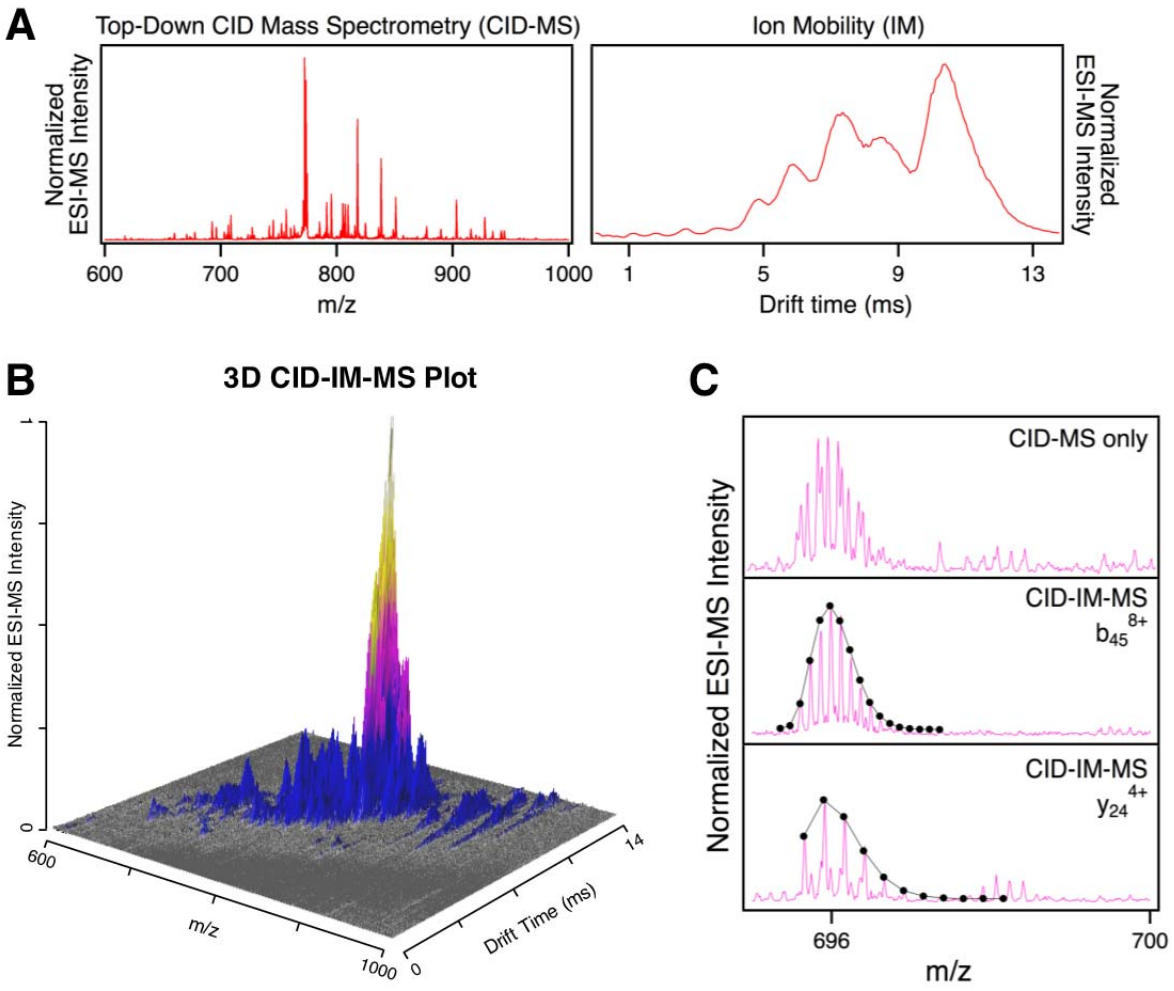

Fig. S6. Principle of top-down CID-IM-MS experiments. (A) Fragmentation is initially achieved by precursor selection and CID in the trap collision cell of the Synapt G2, generating a complex mix of product ions. These fragment ions are then subjected to IMS, providing drift time information for each of the gas phase species, thereby adding a second dimension to the MS/MS spectrum (illustrated in panel B). (C) Representative example of peak assignments made possible by top-down CID-IM-MS of CT-cyt *c*. The initial MS/MS spectrum (top) shows signals that occupy the same *m/z* space; such the data cannot be interpreted. Using IMS, the complex multiplet can be separated into clean isotopic distributions: one corresponding to b_{45}^{8+}, and another to y_{24}^{4+}.

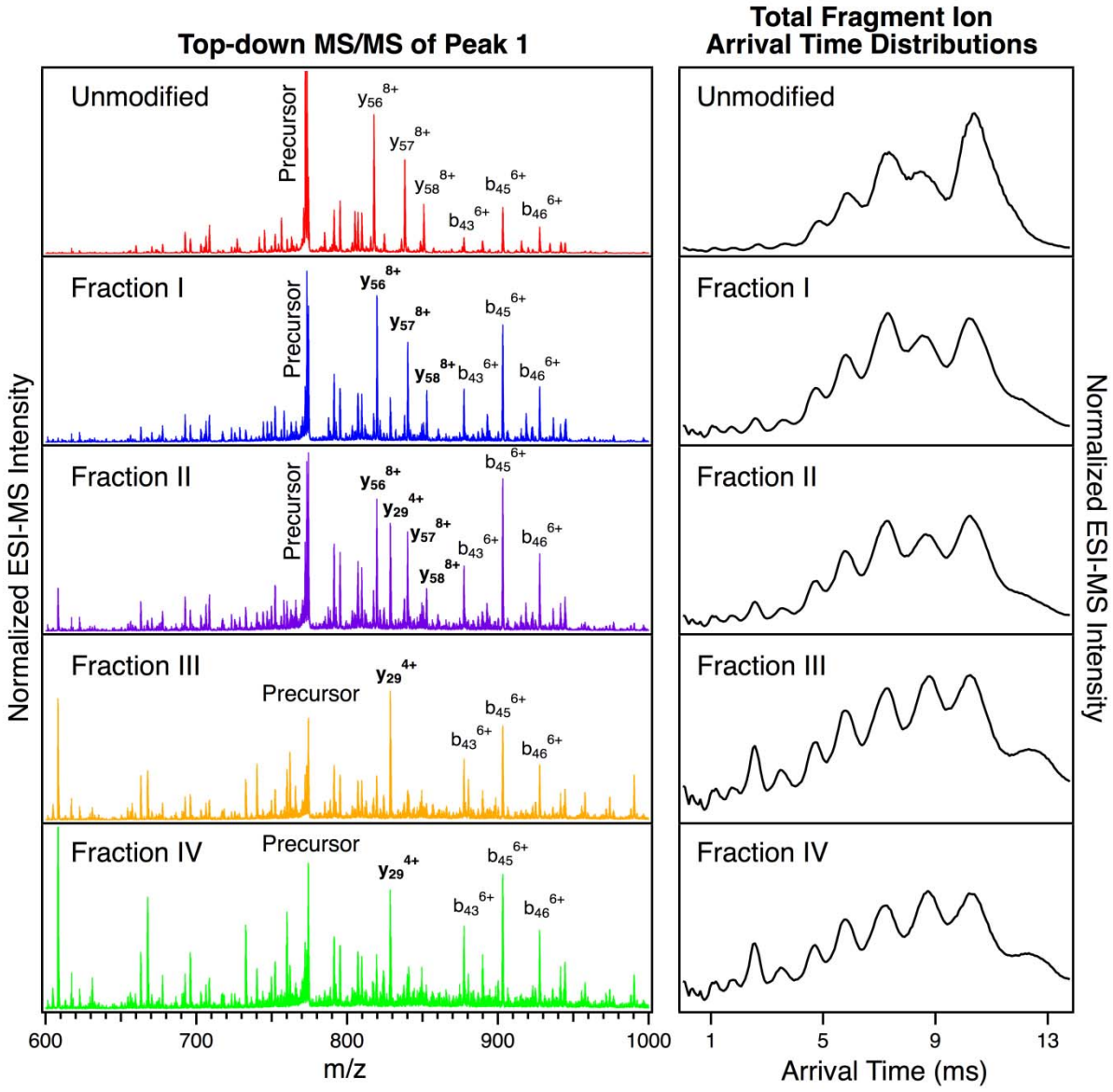

Fig. S7. Representative full CID-IM-MS spectra of peak 1 for all CT-cyt *c* fractions. The CID-IM-MS spectrum of an unmodified control (top, red) is included for comparison. Left: Full MS/MS spectra, with major peaks annotated. Bold labels correspond to fragments that contain an oxidation site (MetO or LysCHO). Right: Total fragment ion IMS arrival time distributions.

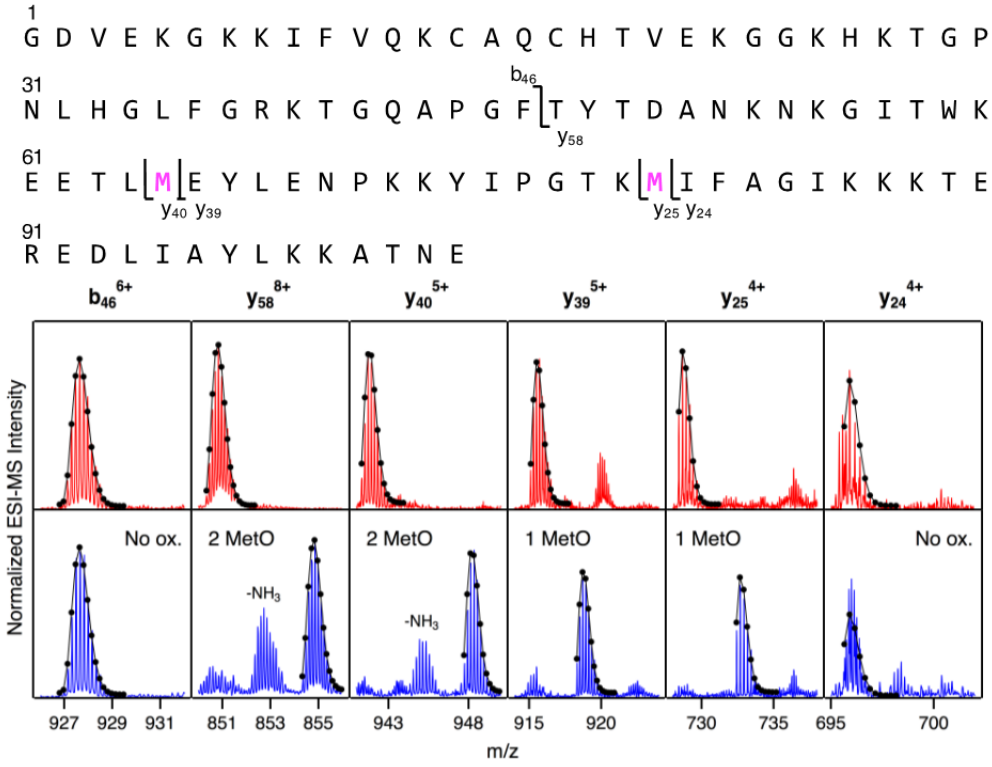

Fig. S8. Representative CID-IM-MS fragment ions to determine the two sites of oxidation in peak 2 of fraction I (+32 Da). Top: Sequence of cyt *c*, with locations of diagnostic fragments labeled. Bottom: Representative fragment ions from an unmodified cyt *c* control (red) and fragment ions of peak 2 of fraction I (blue) overlaid with simulated isotopic envelopes, allowing mapping of the two +16 Da adducts to Met65 and Met80 with single-residue resolution for both.

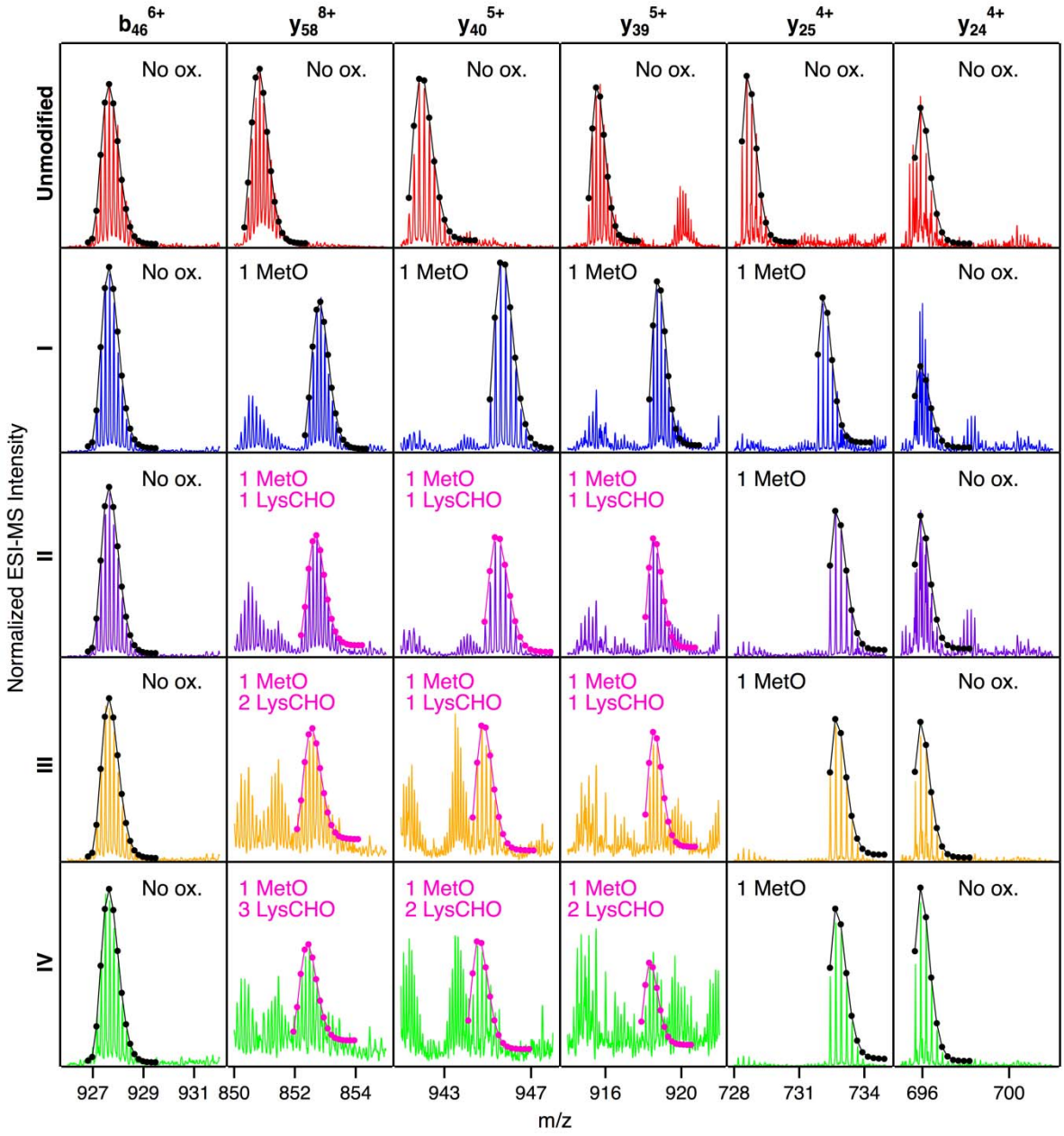

Fig. S9. Diagnostic top-down CID-IM-MS fragment ions of peak 1 for all CT-cyt *c* fractions, highlighting the fact that in all fractions Met80 gets oxidized first. In other words, the first MetO signal in all fractions does *not* originate from heterogeneous Met65/80 oxidation. Each fragment ion is overlaid with a simulated isotopic envelope.

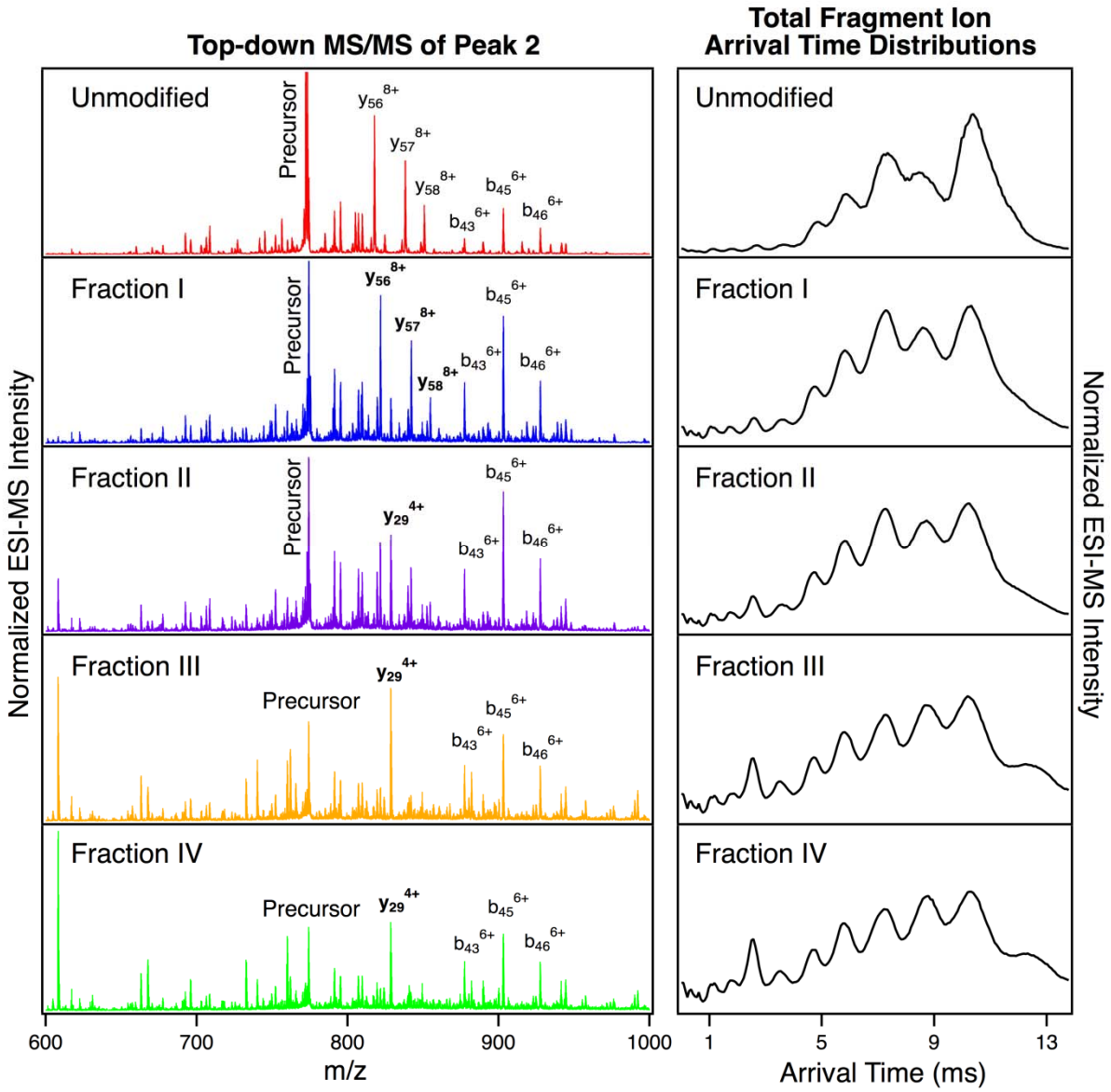

Fig. S10. Representative full CID-IM-MS spectra of peak 2 for all CT-cyt *c* fractions. Data for an unmodified cyt *c* control (top, red) are shown for comparison. Left: Full MS/MS spectra, with major peaks annotated. Bold labels correspond to fragments that contain an oxidation site (MetO or LysCHO). Right: Full total fragment ion IMS arrival time distributions.

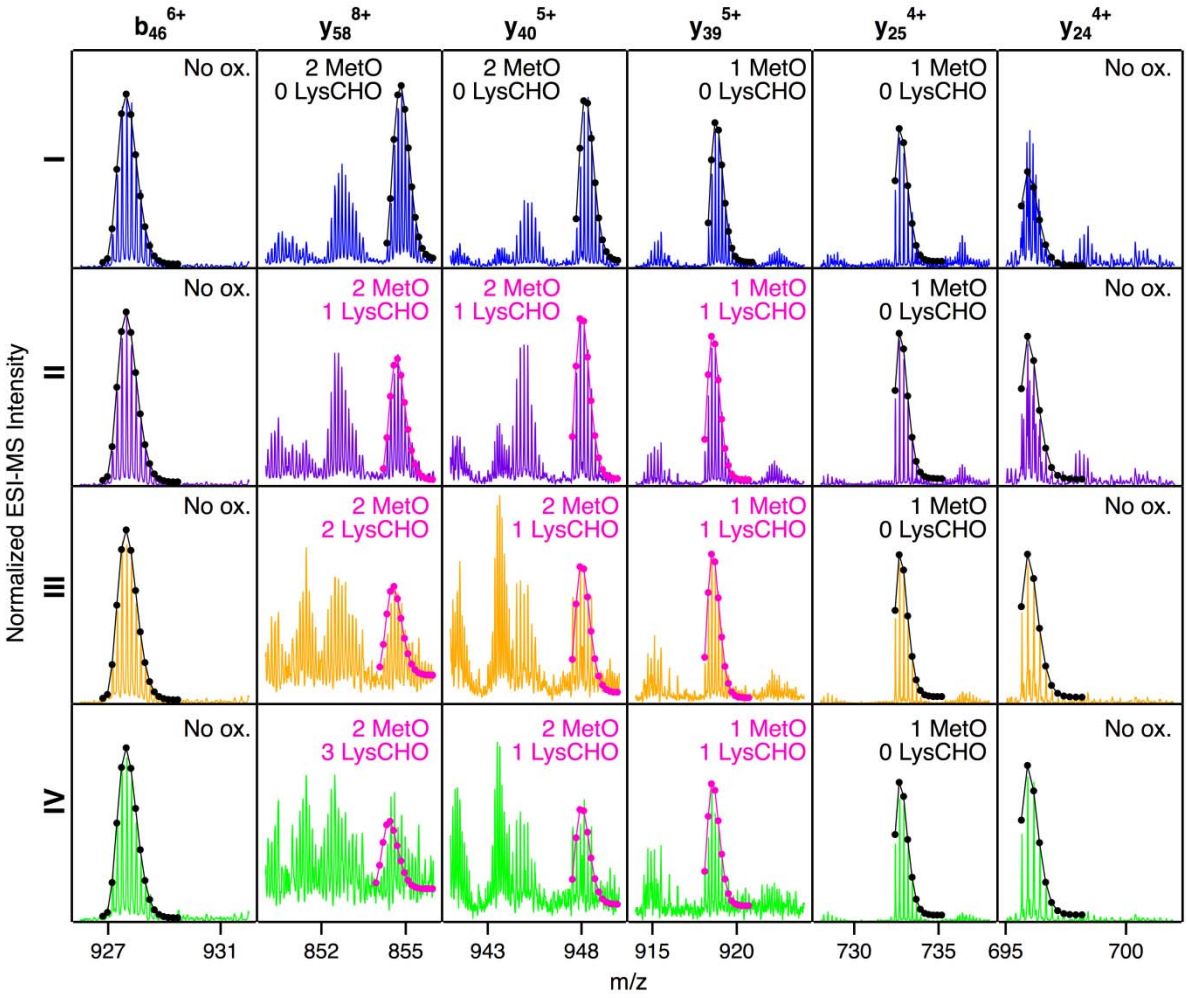

Fig. S11. Diagnostic CID-IM-MS fragment ions of peak 2 for all four CT-cyt c fractions. Each fragment ion is overlaid with a simulated isotopic envelope. Met oxidation for all fractions can be mapped to Met65 and Met80, each with single-residue resolution. The location of LysCHO sites is consistent with the assignments derived for peak 1 (Fig. 5), with some minor differences in fraction IV.

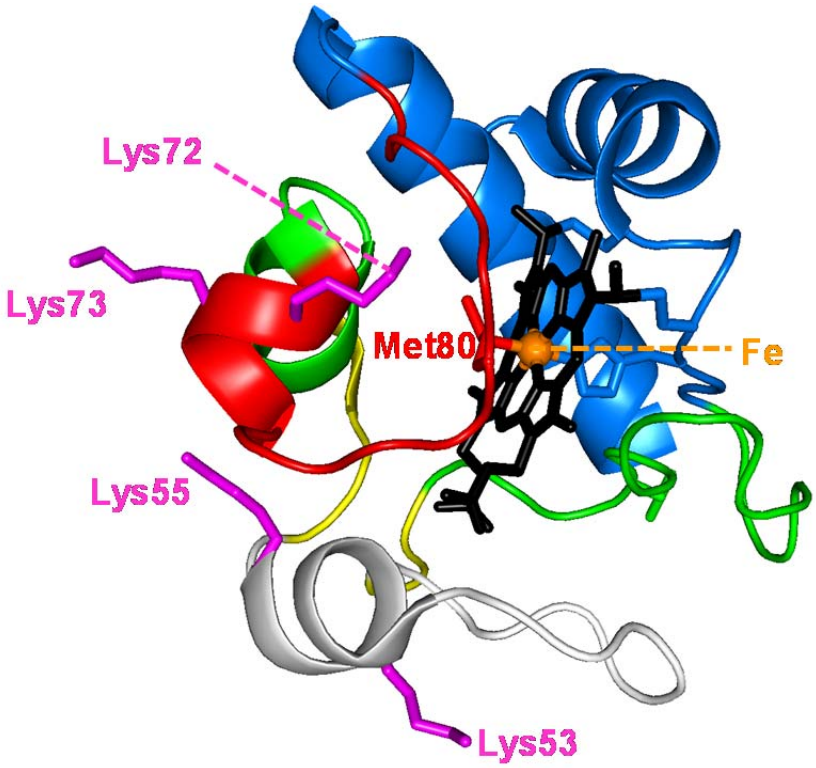

Fig. S12. Foldon structure of cyt *c*.[2] Colors indicate the propensity to undergo transient unfolding: gray (least stable) > red > yellow > green > blue (most stable). Also shown are Lys side chains (magenta) that can act as distal Fe ligands during CT-induced peroxidase activation. Lys72/73 are in the "red" foldon (second-least stable, 71-85 Ω loop). Lys53/55 are in the "gray" foldon (least stable, 40-57 Ω loop). On the basis of our MS results the participation of Lys60 (not shown) in heme ligation cannot be ruled out, but the positioning of Lys60 in the relatively rigid "yellow" foldon renders such a scenario less likely. N.B.: Various terms have been used for the gray foldon; these include "N", "nested yellow", "N-yellow", "infrared", and "black".[2, 3]

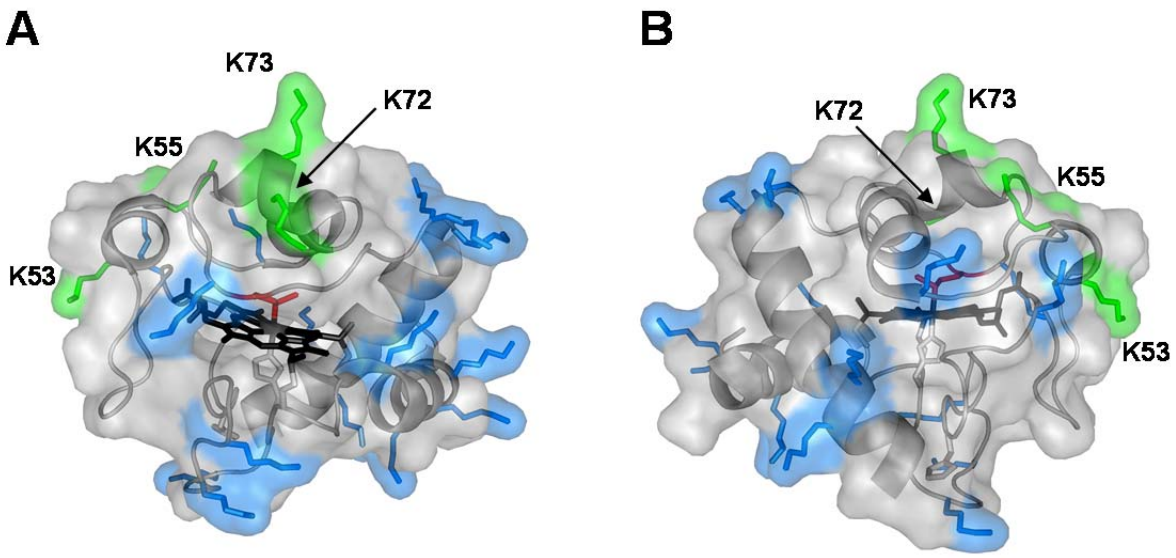

Fig. S13. Crystal structure of native cyt *c* (PDB: 1HRC) depicting all 19 Lys residues. Sites of Lys carbonylation are shown in green, and labeled. All other Lys are shown in blue. (A) Front view. (B) Back view.

	Rate ($\mu M\ s^{-1}$)
Unmod. Control	0.0 ± 0.0
Fraction I	0.5 ± 0.1
Fraction II	0.9 ± 0.2
Fraction III	1.6 ± 0.1
Fraction IV	1.4 ± 0.1

Supporting Table S1. Guaiacol peroxidase kinetics at 100 μM H_2O_2 and 1 μM protein. Rates were measured as the slope of the apparent linear regime in each data set. The reported rates correspond to the formation of tetraguaiacol.

SI References

1. V. Yin, G. S. Shaw and L. Konermann, *J. Am. Chem. Soc.*, 2017, **139**, 15701–15709.
2. M. M. G. Krishna, Y. Lin, J. N. Rumbley and S. W. Englander, *J. Mol. Biol.*, 2003, **331**, 29-36.
3. W. B. Hu, Z. Y. Kan, L. Mayne and S. W. Englander, *Proc. Natl. Acad. Sci. U.S.A.*, 2016, **113**, 3809-3814.